

First-order semi-infinite electron gas model of the quantized carriers of a semiconductor-insulator interface at finite temperatures

T. L. Li*

Department of Applied Physics, National Chia-Yi University, 300 Hsueh-Fu Road, Chiayi 600, Taiwan

T. W. Tang

Department of Electrical and Computer Engineering, University of Massachusetts, Amherst, Massachusetts 01003

(Received 1 June 2001; revised manuscript received 1 April 2002; published 30 August 2002)

In this paper, the first-order semi-infinite electron gas (FOSEG) model of quantized carriers is presented by extending previous theories to take into account both the potential gradient and the vanishing boundary condition. This first-order theory is applicable to the semiconductor-insulator interface at finite temperatures. With the FOSEG, the quantized carrier density at the interface can be calculated without having to explicitly solve the Schrödinger equation.

DOI: 10.1103/PhysRevB.66.075337

PACS number(s): 73.25.+i, 73.20.-r

I. INTRODUCTION

Metal-oxide-semiconductor field-effect transistors (MOSFET's) are vastly utilized in modern electronic devices. In a MOSFET, a thin layer of insulating oxide is sandwiched between the gate metal and the semiconductor as shown in Fig. 1(a) for an *n*-channel MOSFET.^{1,2} When a positive voltage V_G is present across the gate and the substrate, band bending occurs at the semiconductor-insulator interface, and the electrons are attracted towards the interface. These electrons are virtually confined by the infinite barrier of the oxide and the bent conduction band, and are quantized as illustrated in the upper subplot of Fig. 1(b). The quantized carrier density thus formed is illustrated in the lower subplot of Fig. 1(b). The nonvanishing carrier density beyond the classical turning point (labeled as the tunneling tail) is due to the tunneling of lower quantum levels.^{3,4} These quantization effects are important for nanoscale MOSFET's.⁵⁻¹⁰

In the literature, the band bending is sometimes approximated by its tangent line, especially at high electric fields.¹¹ This linear approximation to the conduction band together with the infinite barrier constitutes the triangular potential depicted by the dashed line in the upper subplot of Fig. 1(b).

However, in most basic textbooks of semiconductor device physics, not only the quantization effects but also the infinite barrier were ignored in the carrier density calculation just for simplicity.^{1,2} The carriers near the interface were treated by the homogeneous electron-gas (HEG) model of solid-state physics.¹² In the HEG theory, the carriers are treated as independent particles subject to a constant potential energy in an infinite space. Hence, the HEG model is more appropriate for bulk semiconductors.

For the problems of the semiconductor-insulator interface, the HEG model were modified to take the unpenetrable boundary condition into account. This modification of the homogeneous electron gas was called the modified local-density approximation (MLDA) in Refs. 13 and 14. However, in more modern literature, the local-density approximation usually refers to the approximation used for the exchange and the correlation energy.¹⁵⁻¹⁷ To avoid confu-

sion, the MLDA in Refs. 13 and 14, which treats the correction to the quantized carriers at the semiconductor-insulator interface phenomenologically, is renamed as the semi-infinite electron-gas (SEG) model in this work because the vanishing boundary condition at the unpenetrable interface essentially implies a semi-infinite semiconductor.

In both the HEG model and the SEG model, the potential energy of the electron is independent of the position. Thus, only the zeroth-order position derivative of the potential energy matters in the model. Therefore, both the HEG and the SEG can be considered as a zeroth-order theory. In the quantum-mechanical treatments of the electron gas in this zeroth-order theory, the potential-energy operator commutes with the kinetic-energy operator.^{13,14} Note that both HEG and SEG are finite-temperature models. The temperature is introduced into the models by the Fermi-Dirac distribution.

For the quantized carriers at the semiconductor-insulator interface, the potential energy of the electron is position-dependent due to the band bending caused by the electric field. Under such circumstances, the potential-energy operator and the kinetic-energy operator no longer commute,¹⁸

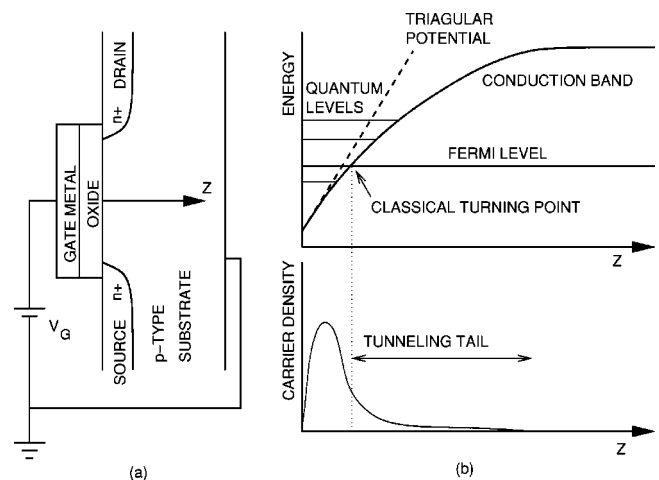


FIG. 1. The device structure of an *n*-channel MOSFET is plotted in (a). Its band diagram and quantized carrier density are plotted in the upper and the lower subplots of (b), respectively.

and, strictly speaking, the zeroth-order theory of the HEG and the SEG no longer holds either.

Moreover, it was reported in the literature that the tunneling tails of the electron wave functions into the band edge introduce a nonvanishing density of states to the conventionally forbidden band gap in the presence of band bending.^{3,4} This tunneling effect cannot be modeled by the HEG and the SEG models because the potential gradient is ignored in both models.

The homogeneous electron gas in the infinite space had been modified to explicitly include the electron potential-energy gradient to first order, leading to the first-order homogeneous electron-gas (FOHEG) approximation.^{19,20} This first-order theory of the electron gas was applicable to the quantized charges of bulk semiconductors at finite temperatures, and was reported to be capable of modeling the electron tunneling effects previously ignored by the conventional zeroth-order theory. However, since the FOHEG does not take the vanishing boundary condition into account, it cannot be applied to the semiconductor-insulator interface.

In this paper, the SEG model is extended, by using some of the techniques developed in the FOHEG for semiconductors at finite temperatures, to explicitly include the electron potential-energy gradient to first order for application to the quantized carriers at the semiconductor-insulator interface. This approximation is called the first-order semi-infinite electron gas (FOSEG) in this work, and is applicable to the semiconductor-insulator interface at finite temperatures because, near the interface, the second- and higher-order derivatives of the potential energy are significantly less important than the first-order derivative. With this approximation, the density of the quantized charges of the semiconductor-insulator interface at finite temperatures can be calculated by an analytic expression without having to explicitly solve the Schrödinger equation.

The four approximations to the electron gas mentioned in this section are the HEG, the SEG, the FOHEG, and the FOSEG. They can be differentiated by the conditions that are taken into account. The conditions are whether the vanishing boundary condition is included and whether the potential gradient is explicitly accounted for. The four approximations and their employed conditions are summarized in Table I.

II. THEORY

A. First-order semi-infinite electron-gas model

The density of the quantized charges of the semiconductor-insulator interface at a finite temperature is usually obtained by first solving the Schrödinger equation for the wave functions and their eigenenergies, and then summing over all the probability density functions weighted by the Fermi-Dirac distribution.¹² Alternatively, the quantized carrier density $n(\vec{r})$ may be calculated by integrating the product of the density of states [DOS, $D(\vec{r}, \varepsilon)$] and the Fermi-Dirac distribution over the energy,^{13,14}

$$n(\vec{r}) = \int d\varepsilon D(\vec{r}, \varepsilon) f(\varepsilon), \quad (1)$$

TABLE I. Four approximations to the electron gas.

	Without potential gradient	With potential gradient
Without vanishing boundary condition	HEG	FOHEG
With vanishing boundary condition	SEG	FOSEG

where $f(\varepsilon) = 1/(1 + e^{\beta(\varepsilon - \varepsilon_F)})$ is the Fermi-Dirac distribution with Fermi energy ε_F and $\beta = 1/kT$ and T is the temperature of the system.

If the insulator is modeled as an unpenetrable barrier located at the $z=0$ plane, then the wave functions vanish at the interface at $z=0$, and the techniques developed in Refs. 13,14 and 19–22, can be utilized to obtain the quantized carrier density using the integral in Eq. (1). Following Refs. 19–23, all second- and higher-order derivatives of the potential energy are neglected. Because only the first-order derivative of the potential energy is retained, this approximation to the quantized carriers of the semiconductor-insulator interface at a finite temperature is called the FOSEG model in this paper.

By the above-mentioned approximation, the approximate DOS at location \vec{r} and energy ε is given by

$$D(\vec{r}, \varepsilon) = \frac{1}{\pi} \left(\frac{m}{2\pi\hbar^2} \right)^{d/2} \int d\omega \frac{1}{\omega^{d/2}} e^{i\omega[\varepsilon - V(\vec{r})]} \times e^{-ia^3\omega^3} [1 - e^{i(m/2\hbar^2)\omega(B\omega + 2z/\omega)^2}], \quad (2)$$

with $a^3 = \hbar^2(\nabla V)^2/24m$ and $B = (\hbar^2/4m)(\partial V/\partial z)$, where d , m , V , and z are the dimensionality, the carrier mass, the potential energy, and the normal distance to the interface, respectively.

The observation of the approximate DOS in Eq. (2) shows that the vanishing boundary condition at $z=0$ is not fulfilled unless $B=0$. Hence, the B term is ignored in the present work to ensure that the boundary condition at $z=0$ is satisfied. With this further approximation, the DOS can be expressed by the following integral:

$$D(\vec{r}, \varepsilon) = \frac{2}{\Gamma\left(\frac{d}{2}\right)} \left(\frac{m}{2\pi\hbar^2} \right)^{d/2} b^{d/2-1} \int_{-\bar{\varepsilon}}^{\infty} dt \text{Ai}(t) \times (\bar{\varepsilon} + t)^{d/2-1} F_d(\alpha[\bar{\varepsilon} + t]) \quad (3)$$

with

$$F_d(s) = 1 - \Gamma\left(\frac{d}{2}\right) (\sqrt{s})^{1-d/2} J_{d/2-1}(2\sqrt{s}), \quad (4)$$

where $b^3 = \hbar^2(\nabla V)^2/8m$, $\alpha = z^2(m|\nabla V|/\hbar^2)^{2/3}$, and $\bar{\varepsilon} = (\varepsilon - V)/b$. Γ , Ai , and $J_{d/2-1}$ are the gamma function, Airy's function, and Bessel function of the first kind, respectively.

The carrier density follows directly from Eqs. (1) and (3), resulting in a double integral. Interchanging the order of the double integral, the carrier density is expressed by

$$n(\vec{r}) = \frac{2}{\Gamma\left(\frac{d}{2}\right)} \left(\frac{m}{2\pi\hbar^2\beta}\right)^{d/2} \int_{-\infty}^{\infty} dt \text{Ai}(t) \int_0^{\infty} ds \times \frac{s^{d/2-1} F_d(\gamma s)}{1 + \exp[s - \beta(bt + \varepsilon_F - V)]}, \quad (5)$$

where $\gamma = mz^2/(\hbar^2\beta)$ and F_d is given by Eq. (4).

B. Relation to other theories

The relations of the FOSEG carrier density in Eq. (5) to other theories will be demonstrated in this section.

It was illustrated in Ref. 19 that the carrier density calculated in Ref. 21 is at a zero temperature, whereas, the method used in Refs. 13, 14, and 19 is a generalization of the zero-temperature formalism to a finite temperature. Since the formulation presented in this section employed methods similar to the latter, the FOSEG carrier density given above is at a finite temperature.

The carrier density for semiconductor-insulator interface at a zero temperature can be obtained from Eq. (5) by letting $T \rightarrow 0$ or $\beta \rightarrow \infty$. The carrier density at this low-temperature limit is, thus, given by

$$n(\vec{r}) \rightarrow \frac{2K_d}{\Gamma\left(\frac{d}{2}\right)} \left(\frac{m}{2\pi\hbar^2}\right)^{d/2} \int_{-\varepsilon}^{\infty} dt \text{Ai}(t) (bt + \varepsilon_F - V)^{d/2}, \quad (6)$$

where $K_d = 2, 1$, and $2/3$ for $d = 1, 2$, and 3 , respectively, and $\varepsilon = (\varepsilon_F - V)/b$. Because the zero-temperature results reported in Eqs. (16) and (17) of Sec. 1.4 of Ref. 21 did not take the interface into account, none of the equations in Ref. 21 can compare with the zero-temperature carrier density in Eq. (6).

At the flat-band limit (∇V and $b \rightarrow 0$) or at the high Fermi-level limit ($\varepsilon_F \gg V$), Eq. (5) suggests that the integrand of the inner integral over s be independent of t . Hence, the carrier density at any of these two limits becomes

$$n(\vec{r}) \rightarrow \frac{2}{\Gamma\left(\frac{d}{2}\right)} \left(\frac{m}{2\pi\hbar^2\beta}\right)^{d/2} \int_0^{\infty} ds \frac{s^{d/2-1} F_d(\gamma s)}{1 + \exp[s - \beta(\varepsilon_F - V)]}. \quad (7)$$

For the dimensionality $d = 3$, the above carrier density expression can be shown to be identical with Eq. (20) of Ref. 13. (This is not surprising because, in Ref. 13, the gradient of the potential energy is completely ignored to facilitate the commutation of the potential-energy and the kinetic-energy operators.) Therefore, the carrier density obtained by the FOSEG of this work indeed reduces to the flat-band equation

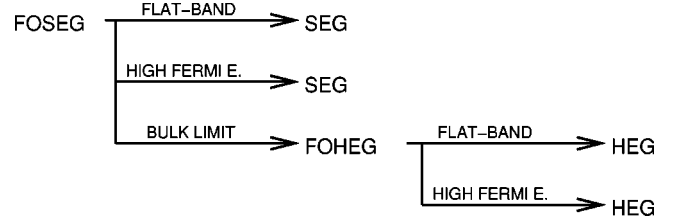


FIG. 2. The relations of the FOSEG to other theories are summarized in this chart.

of the SEG in Ref. 13 as the potential-energy gradient diminishes. This reduction will also be confirmed numerically in the following section.

At the large normal distance limit (z and $\gamma \rightarrow \infty$), the FOSEG carrier density expression in Eq. (5) can be easily shown to reduce to

$$n(\vec{r}) \rightarrow 2 \left(\frac{m}{2\pi\hbar^2\beta}\right)^{d/2} \int_{-\infty}^{\infty} dt \text{Ai}(t) \mathcal{F}_{d/2-1}[\beta(bt + \varepsilon_F - V)], \quad (8)$$

where $\mathcal{F}_j(x) = 1/\Gamma(j+1) \int_0^{\infty} dt t^j / (1 + e^{t-x})$ is the Fermi-Dirac integral²⁴ of order j and argument x . Equation (8) is the FOHEG carrier density reported in Ref. 19 for bulk semiconductors without insulating interfaces. The result for this limit is consistent with the physical intuition that the effect of the interface on the carrier density decreases as the location \vec{r} is farther from the interface. Hence, this limit is also termed the bulk limit.

The relations of the FOSEG of this work to other finite-temperature theories it reduces to are summarized in Fig. 2.

III. RESULT AND DISCUSSION

In contrast to the SEG theory, the FOSEG theory of this work explicitly takes the first-order gradient of the potential energy into account.

In order to study the validity of both approximate methods, the DOS and the carrier density are calculated by the FOSEG and by the SEG, and are compared with the exact solution to the triangular potential of

$$V(\vec{r}) = \begin{cases} eFz & \text{if } z > 0 \\ \infty & \text{if } z < 0, \end{cases} \quad (9)$$

where e is the magnitude of the electron charge, F is the electric field, and z is the normal distance to the interface. Note that the zero-potential-energy reference point is at $z = 0$. As shown in Fig. 1, the triangular potential had been used as an approximation to the quantization of carriers at the semiconductor-insulator interface, and the exact DOS and the exact carrier concentration of the triangular potential are available in Ref. 11.

In all of the calculations of this work, the electron mass is taken to be the effective mass of the silicon electron, $m = 1.18m_0$, where m_0 is the electron rest mass, and the temperature is taken to be at 300 K. Only three-dimensional ($d = 3$) results are presented in this section.

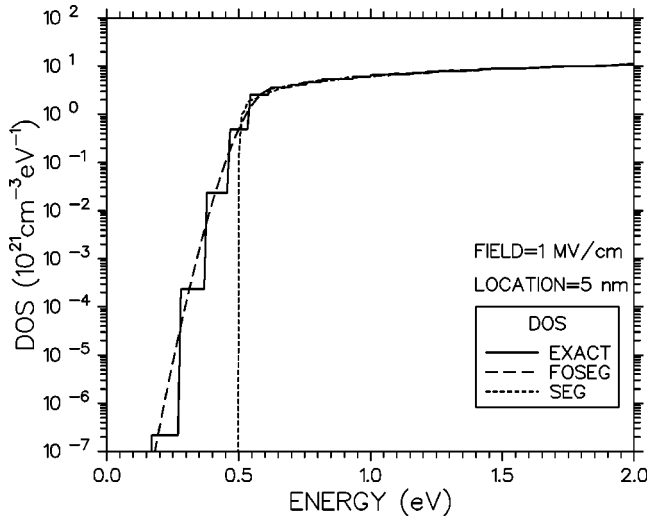


FIG. 3. The DOS of a triangular potential with the electric field of 1 MV/cm is plotted versus energy at location $z=5$ nm. The DOS's obtained by the exact solution, the FOSEG, and the SEG are plotted in solid, dashed, and dotted lines, respectively.

The DOS of the triangular potential obtained by the exact solution, by the FOSEG in Eq. (5), and by the SEG in Eq. (7) are plotted in solid, dashed, and dotted lines, respectively, for the electric field of 1 MV/cm in Figs. 3 and 4. Similar results were reported for a much lower electric field of 0.05 MV/cm in Figs. 2–4 of Ref. 13, using the SEG model. The FOSEG of this work is a higher-order approximation than the SEG, and is expected to perform better than the SEG at high electric fields. Therefore, a high electric field of 1 MV/cm (near the edge of material breakdown²) is deliberately chosen for presentation. Moreover, as shown in Eq. (7) and the text following it, the FOSEG reduces to the SEG at low fields. Hence, a comparison between these two models at low field

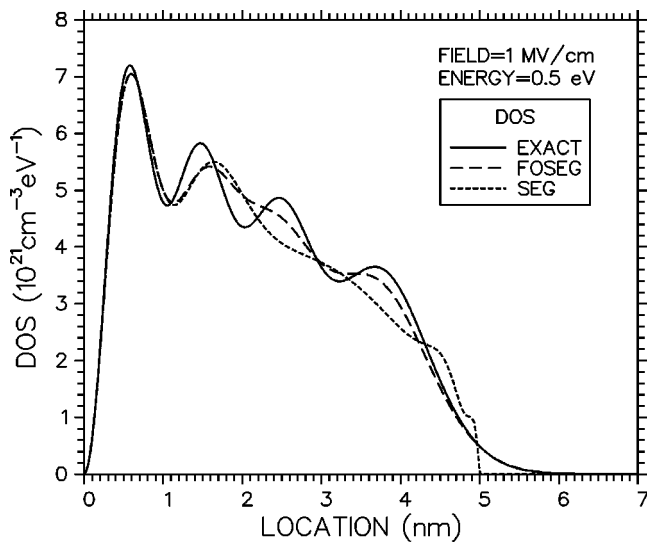


FIG. 4. The DOS of a triangular potential with the electric field of 1 MV/cm is plotted versus location at energy $\varepsilon=0.5$ eV. The DOS's obtained by the exact solution, the FOSEG, and the SEG are plotted in solid, dashed, and dotted lines, respectively.

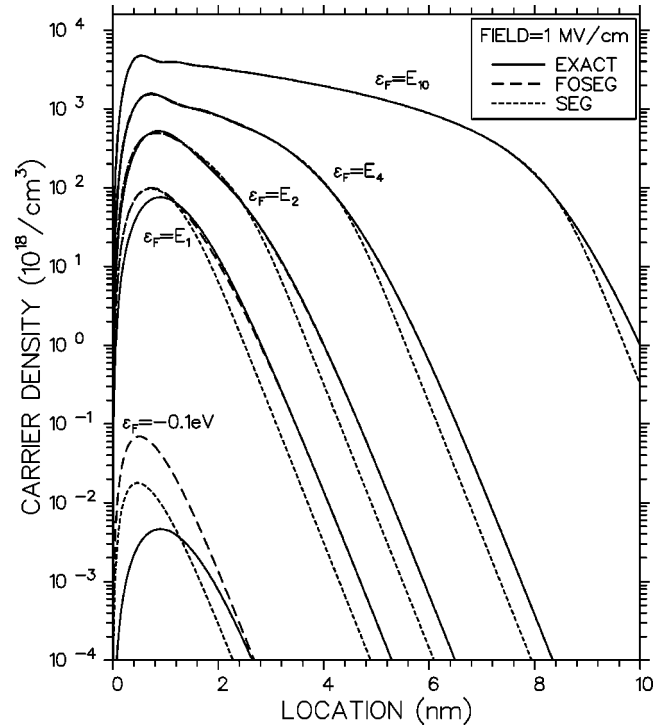


FIG. 5. The carrier density of a triangular potential with the electric field of 1 MV/cm is plotted for Fermi levels $\varepsilon_F = -100$, 160.41 (E_1), 280.45 (E_2), 465.60 (E_4), and 880.11 (E_{10}) meV. The carrier densities obtained by the exact solution, the FOSEG, and the SEG are plotted in solid, dashed, and dotted lines, respectively.

is trivial and is not shown. The DOS at other electric fields is qualitatively similar and is, thus, not shown either.

In Fig. 3, the DOS is plotted as a function of energy at location $z=5$ nm in logarithmic scale. The DOS obtained by the conventional SEG vanishes as the energy ε is below the conduction-band edge at $V(z=5 \text{ nm})=0.5$ eV. However, the exact solution exhibits nonvanishing DOS below the band edge.

In Fig. 4, the DOS is plotted as a function of location for energy $\varepsilon=0.5$ eV in linear scale. The DOS predicted by the conventional SEG vanishes beyond the classical turning point at $z=5$ nm. But, the exact results exhibit a nonvanishing tail beyond the classical turning point.

The nonvanishing DOS below the band edge and beyond the classical turning point illustrated in Figs. 3 and 4, respectively, is due to the quantum-mechanical tunneling of wave functions, at the presence of the electric field, into the semiconductor beyond the turning point. The tunneling effectively lowers the conduction-band edge, and consequently reduces the band gap.^{3,4} The conventional SEG theory cannot model this tunneling effect because of the explicit negligence of the potential gradient in its formalism. On the contrary, the FOSEG theory of this work accounts for the potential gradient to the first order, and is more capable of modeling the tunneling effects than the SEG theory.

The carrier densities as functions of the location are plotted in Figs. 5, 6, and 7 for the triangular potentials with electric field $F=1$, 0.5, and 0.1 MV/cm, respectively. In each figure, the carrier densities for Fermi levels at

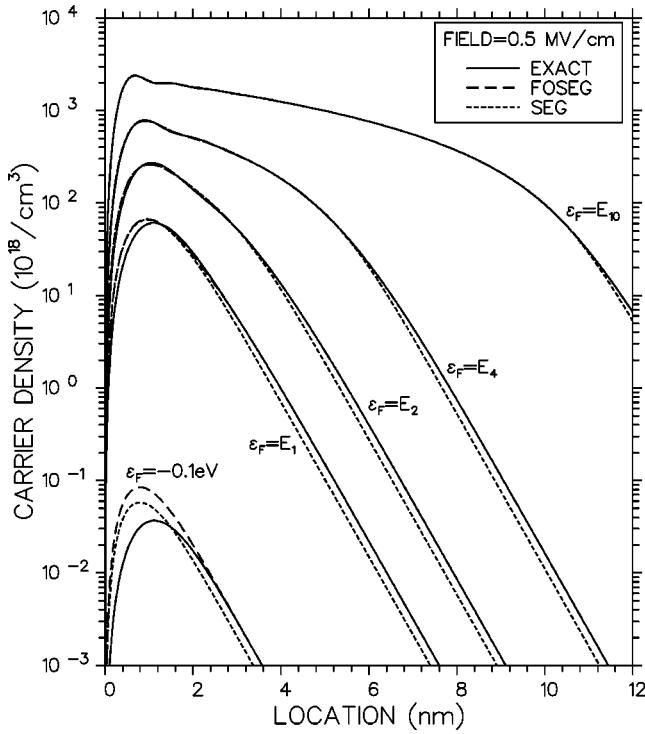


FIG. 6. The carrier density of a triangular potential with the electric field of 0.5 MV/cm is plotted for Fermi levels $\varepsilon_F = -100$, 101.05 (E_1), 176.68 (E_2), 293.31 (E_4), and 554.44 (E_{10}) meV. The carrier densities obtained by the exact solution, the FOSEG, and the SEG are plotted in solid, dashed, and dotted lines, respectively.

−0.1 eV, the first (E_1), the second (E_2), the fourth (E_4), and the tenth (E_{10}) eigenenergies of the triangular barrier are depicted. (As noted in the text following Eq. (9), the zero-potential-energy reference is at the minimum of the triangular potential. Negative Fermi energies simply mean those below the potential minimum.) The eigenenergies of the above-mentioned eigenlevels are different for the triangular barrier under different electric fields, and are tabulated in Table II. The carrier densities obtained by the exact solution, by the FOSEG, and by the SEG are plotted in solid, dashed, and dotted lines, respectively, in Figs. 5, 6, and 7. One of the main differences between the FOSEG of the present work and the SEG of Ref. 13 is that the former is capable of modeling the tunneling tail of carrier density beyond the classical turning point. In order to illustrate the tunneling carrier density, the logarithmic scale is used in Figs. 5, 6, and 7.

The quantized carriers at the interface under a strong electric field of 1 MV/cm is plotted in Fig. 5. Three features are observed in this carrier density plot.

First, at lower Fermi energy such as $\varepsilon_F = -0.1$ eV and E_1 , both FOSEG and SEG greatly deviate from the exact carrier density. (Although the FOSEG agrees better with the exact carrier density at the tail than the SEG, it is not of much significance because the peak concentration is off by almost an order of magnitude.) It is found that, at the electric field of 1 MV/cm, there must be at least four quantum levels below the Fermi level for the FOSEG results to be suffi-

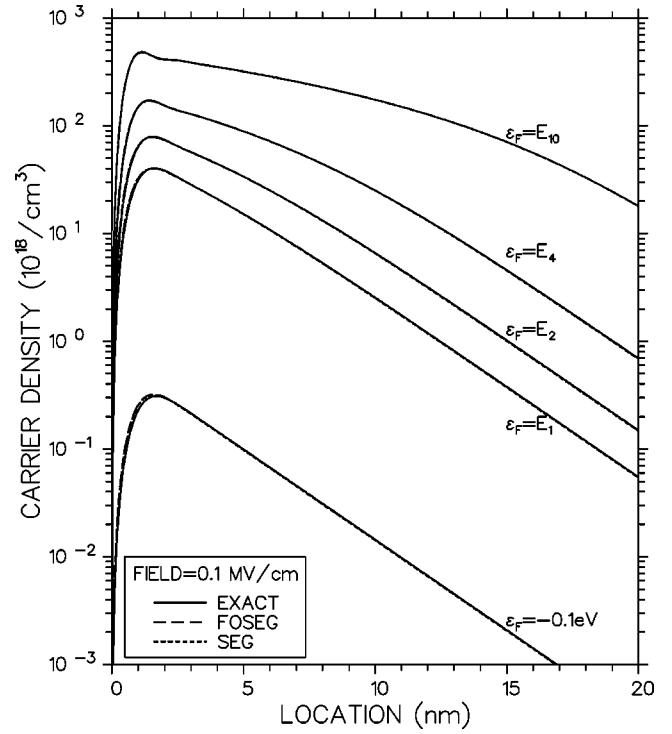


FIG. 7. The carrier density of a triangular potential with the electric field of 0.1 MV/cm is plotted for Fermi levels $\varepsilon_F = -100$, 34.56 (E_1), 60.42 (E_2), 100.31 (E_4), and 189.62 (E_{10}) meV. The carrier densities obtained by the exact solution, the FOSEG, and the SEG are plotted in solid, dashed, and dotted lines, respectively.

ciently close to the exact solution. At Fermi energy $\varepsilon_F = E_4$ and E_{10} , the FOSEG lines are indistinguishable from the exact lines in the figure.

Second, the FOSEG results with successively higher Fermi energy ($\varepsilon_F = -0.1$ eV, E_1 , E_2 , E_4 , and E_{10}) show that systems with more quantum levels below the Fermi energy better approach the exact solution.

Third, at the classical turning point associated with the Fermi energy [given by the location $z_F = \varepsilon_F / (eF)$], the carrier density obtained by the conventional SEG starts to deviate more significantly from the exact solution, but the FOSEG well matches the exact results. This is due to the fact that the tunneling of the wave functions beyond the classical turning point is included in the formalism of the FOSEG as illustrated in Figs. 3 and 4.

Figure 6 shows the carrier density at the electric field of 0.5 MV/cm. The three features observed in Fig. 5 and stated in the above paragraphs for the field of 1 MV/cm also hold qualitatively for this field.

TABLE II. Eigenenergies of a triangular potential

Field (MV/cm)	E_1 (meV)	E_2 (meV)	E_4 (meV)	E_{10} (meV)
F=1.0	160.41	280.45	465.60	880.11
F=0.5	101.05	176.68	293.31	554.44
F=0.1	34.56	60.42	100.31	189.62

The carrier density at a lower electric field of 0.1 MV/cm is shown in Fig. 7. The curves for the exact solution, the FOSEG, and the SEG are almost indistinguishable. This is a numerical confirmation of SEG being the flat-band limit of the FOSEG as indicated in the text following Eq. (7).

From Figs. 5, 6, and 7, it found that the system must have enough number of quantum levels below the Fermi level for the FOSEG to sufficiently approach the exact solution, and that the number of quantum levels below the Fermi energy increases with the electric field (for example, four and two levels for $F = 1$ and 0.1 MV/cm, respectively). Hence, it is claimed in this paper that, under all practical strengths of the electric field, the FOSEG is a good approximation to the exact solution if there are at least four quantum levels below the Fermi level.

IV. CONCLUSIONS

The semi-infinite electron gas (SEG) in the literature is extended to include the first-order derivative of the electron potential energy, resulting in the first-order semi-infinite electron gas (FOSEG) of this work. The FOSEG is applicable to the quantized carriers of semiconductor-insulator interfaces at finite temperatures.

With the FOSEG, the density of states and the carrier

density are given by the analytic expressions in Eqs. (3) and (5), respectively. These equations reduce to the SEG results reported in the literature as the potential gradient gradually diminishes.

In contrast to the SEG, the FOSEG explicitly includes the potential-energy gradient in its formalism, and is capable of accounting for the tunneling of electron wave functions beyond the classical turning point. Hence, the nonvanishing density of states below the band edge at the presence of the band bending can be modeled by the FOSEG of this work, but was completely ignored by the SEG.

It is found that the FOSEG carrier density better matches the exact solution for systems with more quantum levels below the Fermi level. Moreover, at locations beyond the classical turning point associated with the Fermi energy, the carrier density obtained by the FOSEG matches the exact solution better than the SEG because of its explicit inclusion of the potential-energy gradient in the formulations of the FOSEG.

ACKNOWLEDGMENT

T.L.L. acknowledges the support of the National Science Council of Taiwan through Grants Nos. NSC90-2215-E-415-001 and NSC89-2215-E-415-001.

*Corresponding author.

Email address: quantum@mail.ncyu.edu.tw

URL: <http://mail.ncyu.edu.tw/quantum>

¹R. F. Pierret, *Semiconductor Device Fundamentals* (Addison-Wesley, Reading, MA, 1996).

²S. M. Sze, *Physics of Semiconductor Devices*, 2nd ed (Wiley, New York, 1981),.

³J.H. Davies and J.W. Wilkins, *Phys. Rev. B* **38**, 1667 (1988).

⁴J.R. Lowney and H.S. Bennett, *J. Appl. Phys.* **65**, 4823 (1989).

⁵F. Chirico, F.D. Sala, A.D. Carlo, and P. Lugli, *Physica B* **272**, 546 (1999).

⁶A.S. Spinelli, A. Benvenuti, and A. Pacelli, *IEEE Trans. Electron Devices* **45**, 1342 (1998).

⁷Y. Taur, Y.-J. Mii, D.J. Frank, H.-S. Wong, D.A. Buchanan, S.J. Wind, S.A. Rishton, G.A. Sai-Halasz, and E.J. Nowak, *IBM J. Res. Dev.* **39**, 245 (1995).

⁸Y. Taur *et al.*, *Proc. IEEE* **85**, 486 (1997).

⁹Y. Taur, *IEEE Spectrum* **36**(7), 25–29 (1999).

¹⁰H.-S.P. Wong, D.J. Frank, P.M. Solomon, C.H.J. Wann, and J.J. Welser, *Proc. IEEE* **87**, 537 (1997).

¹¹A.P. Gnadinger and H.E. Talley, *Solid-State Electron.* **13**, 1301 (1970).

¹²N. W. Ashcroft and N. D. Mermin, *Solid State Physics* (Saunders, Philadelphia, 1976).

¹³G. Paasch and H. Ubensee, *Phys. Status Solidi B* **113**, 165 (1982).

¹⁴G. Paasch and H. Ubensee, *Phys. Status Solidi B* **118**, 255 (1983).

¹⁵R. M. Dreizler and E. K. U. Gross, *Density Functional Theory—An Approach to the Quantum Many-Body Problem* (Springer-Verlag, Berlin, 1990).

¹⁶X. Gonze, P. Ghosez, and R.W. Godby, *Phys. Rev. Lett.* **74**, 4035 (1995).

¹⁷I.I. Mazin and D.J. Singh, *Phys. Rev. B* **57**, 6879 (1998).

¹⁸J. J. Sakurai, *Modern Quantum Mechanics* (Benjamin/Cummings, Menlo Park, CA, 1985).

¹⁹T.L. Li, *Phys. Rev. B* **65**, 193203 (2002).

²⁰T.L. Li, *Chin. J. Phys. (Taipei)* **39**, 453 (2001).

²¹V.W. Macke and P. Rennert, *Ann. Phys. (N.Y.)* **12**, 84 (1963a).

²²V.W. Macke and P. Rennert, *Ann. Phys. (N.Y.)* **12**, 32 (1963b).

²³T.L. Li and T.W. Tang, *Chin. J. Phys. (Taipei)* **40**, 48 (2002).

²⁴M. Goano, *Solid-State Electron.* **36**, 217 (1993).